Available online at www.sciencedirect.com
SCIENCE DIRECT
Thin Solid Films 510 (2006) 222–228
thin solid films
www.elsevier.com/locate/tsf

Effect of the microstructure of Si_3N_4 on the adhesion strength of TiN film on Si_3N_4

Young-Gu Kim [a], Junichi Tatami [b], Katsutoshi Komeya [b], Do Kyung Kim [a,*]

[a] Department of Materials Science and Engineering, Korea Advanced Institute of Science and Technology (KAIST), Yusong, Taejon 305-701, Korea
[b] Graduate School of Environment and Information Sciences, Yokohama National University, Yokohama, Japan

Received 12 October 2004; received in revised form 5 October 2005; accepted 21 December 2005
Available online 7 February 2006

Abstract

The effect of the microstructure of silicon nitride, which was used as a substrate, on the adhesion strength of physical vapor deposited TiN film on Si_3N_4 was investigated. Silicon nitride substrates with different microstructures were synthesized by controlling the size (fine or coarse), the phase (α or β) of starting Si_3N_4 powder, and sintering temperature. The microstructure of Si_3N_4 was characterized in terms of grain size, aspect ratio of the elongated grain, and β-to-α phase ratio. For a given chemical composition but different mechanical properties, such as toughness, elastic modulus, and hardness of Si_3N_4 were obtained from the diverse microstructures. Hertzian indentation was used to estimate the yield properties of Si_3N_4, such as critical loads for yield (P_y) and for ring cracking (P_c). The effect of the microstructure of Si_3N_4 on adhesion strength evaluated by scratch test is discussed. TiN films on Si_3N_4 showed high adhesion strengths in the range of 80–140 N. Hardness and the P_y of Si_3N_4 substrate were the primary parameters influencing the adhesion strength of TiN film. In TiN coating on Si_3N_4, substrates with finer grain sizes and higher α phase ratios, which show high hardness and high P_y, were suitable for higher adhesion strength of TiN film.

PACS: 68.60B; 46.30.P; 81.40.N; 81.05.J, M
Keywords: Adhesion; Hardness; Titanium nitride; Silicon nitride

1. Introduction

TiN coatings have a high elastic modulus, hardness, good wear resistance, and a low frictional coefficient. These characteristics enable TiN to be applicable as protective and functional coating to increase the life of machining tools [1–5] or to diffuse or act as an oxidation barrier in semiconductor devices [6–8]. Strong adhesion is necessary to obtain high performing TiN. A number of factors have been found to influence adhesion strength between the coating and substrate in Physical Vapor Deposition system. These include coating thickness, substrate hardness, internal stress, and so on [9–15].

Silicon nitride is one of the most successful structural ceramics over the last two decades. Silicon nitride possesses well-balanced mechanical properties, such as a high strength of up to 1 GPa, a high elastic modulus of 330 GPa, and a hardness of 23 GPa. The properties of Si_3N_4 strongly depend on its microstructure, in terms of grain size, β-to-α phase ratio, aspect ratio of elongated β grains, and grain boundary second phase [16–19]. The major application fields of Si_3N_4 have been engine components and cutting tools, and have recently extended to the bearings for high speed or severe environments [20]. However, the relatively high frictional coefficient and high manufacturing cost of Si_3N_4 bearings limit a wider application to various fields.

In this study, as a representative of hard coating material, TiN coatings have been coated on Si_3N_4 by the PVD process, and the adhesion strength of the TiN film was characterized. Previously, TiN dispersed Si_3N_4 composites have been studied [21–23], but TiN coated Si_3N_4 has rarely been reported. In this work, the effects of the microstructure of Si_3N_4 substrate on the adhesion strength of PVD TiN coating on Si_3N_4 were investigated. Silicon nitride substrates with different microstructures but the same composition were fabricated by controlling the size and the phase of the Si_3N_4 starting powder and sintering

* Corresponding author. Tel.: +82 42 869 4118; fax: +82 42 869 3310.
E-mail address: dkkim@kaist.ac.kr (D.K. Kim).

0040-6090/$ - see front matter © 2005 Elsevier B.V. All rights reserved.
doi:10.1016/j.tsf.2005.12.304

temperature. This study aims to propose the optimum Si_3N_4 microstructure for the best performance of TiN coated Si_3N_4 for various applications including bearings.

2. Experimental details

Physical vapor deposited TiN films on Si_3N_4 ceramic substrates were fabricated, the properties of the substrate and TiN film were evaluated, and adhesion strengths were measured, as indicated in Fig. 1. For the preparation of the ceramic substrate, three kinds of Si_3N_4 powder were used: 0.3 μm fine powder with α phase (UBE-SN-10, Tokyo, Japan), 1.0 μm coarse powder with α phase (UBE-SN-E3, Tokyo, Japan), and 3.0 μm β powder (KSN-80SP, ShinEtsu, Tokyo, Japan). As sintering additives, 5 wt.% Y_2O_3 (Fine Grade, H.C. Starck GmbH, Goslar, Germany), 2 wt.% Al_2O_3 (AKP50, Sumitomo Chemical Co. Ltd., Tokyo, Japan), and 1 wt.% MgO (High Purity, Baikowski Co., NC, USA) were added to the powder mixture. Ball milling was carried out for 24 h with a ZrO_2 ball in 2-PrOH to obtain uniform mixing. After drying in a convection oven at 50 °C for 6 h, the mixed powders were granulated by sieving with a 60-mesh screen.

Hot pressing (Thermal Technology Inc., ASTRO group 1400, CA, USA) was conducted to sinter Si_3N_4 powder under the conditions of the uniaxial compression of 25 MPa in a 1 atm N_2 atmosphere at 1600, 1700, and 1800 °C for 1 h. The heating rate was 25 °C/min and temperature was measured by pyrometer (TR-630A, Minolta, Japan). The sintered specimen was 20 mm in diameter and 3 mm in thickness. After successive polishings with 6, 3, and 1 μm diamond paste, Si_3N_4 was plasma etched to observe its microstructure. During plasma etching, the flow rate of CF_4, and O_2 was 40 and 80 sccm, respectively. A chamber pressure of 34.55 Pa was maintained, and 80 W of RF power was applied for 10 min. The average size and aspect ratio of Si_3N_4 grains were measured by an image analyzer (Bioscan OPTIMAS 4.1, Bioscan Inc., Edmonds, WA, USA). The phase ratio of β-to-α was determined by relative peak intensity ratio obtained from α and β phase according to Gazzara and Messier procedure [24], and density was measured by Archimedes method.

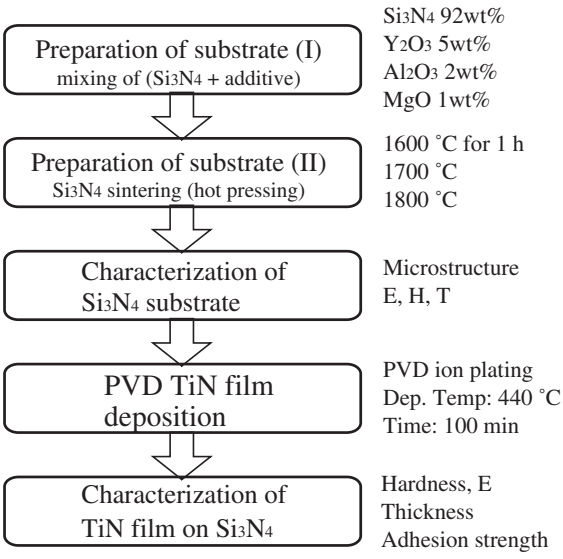

Fig. 1. The flow chart of synthesis of Si_3N_4 substrates and deposition of the PVD TiN film on Si_3N_4.

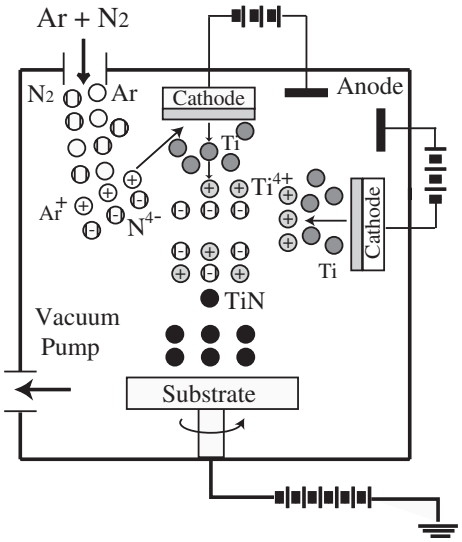

Fig. 2. The schematic design of the cathodic arc ion plating system for TiN deposition. Substrate holder was rotated at a speed of 5 rpm to get uniform TiN thickness on the whole substrate area.

Elastic modulus of Si_3N_4 was evaluated by the impulse excitation of vibration [25], and fracture toughness was obtained by measuring the length of radial cracks after Vickers indentation [26]. A Hertzian indentation with a WC spherical ball of 1.98 mm in radius was introduced on a polished Si_3N_4 surface to determine the critical load for yield P_y, and the critical load for ring cracking, P_c. The critical load for yield is defined as the initial load for inducing surface indentation impression [27]. Load was applied from 700 to 3000 N at an interval of 100 N, and cross-head speed remained constant at 0.5 mm/min. After indentation, the surface of the Si_3N_4 was examined by optical microscopy with Nomarski illumination.

The TiN was deposited by arc ion plating. Fig. 2 shows the schematics of arc ion plating equipment. Before placing in the deposition chamber, the Si_3N_4 substrates were cleaned in TCE (trichloloethylene), were heated to 440 °C; Ti ion cleaning continued for 10 min. During deposition, working pressure was maintained at 0.97 Pa. Table 1 shows processing parameters in detail.

The crystal structure of the TiN coating was confirmed by X-Ray Diffraction, and TiN thickness was measured by Scanning Electron Microscope in a cross-sectional view. The elastic modulus and hardness of TiN coating were estimated by nano indentation (Triboscope, Hysitron Inc., MN, USA). Load was applied from 1 to 10 mN for 20 data points, and then the average hardness and elastic modulus were calculated. Adhesion strength of TiN on Si_3N_4 was measured by a scratch tester (CSEM, CSEM Inc., Swiss). A diamond cone with a 200 μm tip radius was used for scratch test at a loading rate of 100 N/min and a scratch speed of 10 mm/min. Adhesion strength, L_c,

Table 1
The processing parameters for TiN deposition by ion plating

Parameters	Details
Basic chamber pressure (Pa)	7.97×10^{-4}
Working pressure (Pa)	0.97
Substrate temperature (°C)	440
Substrate bias (V)	−100
Current (A)	4.6
Deposition time (min)	100
Deposition rate (nm/min)	10
Flowing rate of N_2 (sccm)	95

was determined by the signals of acoustic emission, the frictional coefficient, and by the critical load for film failure with optical microscopy.

3. Results and discussion

3.1. Microstructure and characteristics of the Si_3N_4 substrate

The microstructure of silicon nitride can be controlled by a variety of processing parameters, such as sintering temperature and time, the chemical composition of sintering additives, size, distribution, and the β-to-α ratio of Si_3N_4 starting powder. Fig. 3 compares the microstructures of silicon nitride substrates prepared from different sintering temperatures and different starting powders. Fig. 3(a)−(c) indicates microstructure of the Si_3N_4 with a fine starting powder with α phase sintered at 1600, 1700, and 1800 °C, respectively. Fig. 3(d)−(f) shows the Si_3N_4 sintered at 1600, 1700, and 1800 °C with a coarse α Si_3N_4 powder. Fig. 3(g)−(i) expresses the Si_3N_4 sintered at 1600, 1700, and 1800 °C with a starting powder of β phase.

Table 2
The characterization of Si_3N_4 substrates

Si_3N_4 specimen code	Starting powder[a]	Sintering temp. (°C)	Grain size (μm)	β/α ratio	Aspect ratio	Fraction of elongated β (v/o)	Density (g/cm^3)
F1	AF	1600	0.23	0.42	5.2	0.10	3.26
F2	AF	1700	0.28	0.84	5.2	0.22	3.25
F3	AF	1800	1.13	1.00	5.2	0.27	3.22
C1	AC	1600	0.43	0.09	NA[b]	NA[b]	3.24
C2	AC	1700	0.48	0.15	3.4	0.05	3.24
C3	AC	1800	1.21	0.38	5.5	0.26	3.22
B1	B	1600	2.20	1.00	3.2	0.24	3.00
B2	B	1700	2.46	1.00	2.2	0.27	3.20
B3	B	1800	3.35	1.00	2.7	0.38	3.19

[a] AF, AC, and B denote a fine (0.3 μm) α phase, a coarse (1.0 μm) α phase, and β phase (3.0 μm), respectively.
[b] C1 specimen shows equiaxed microstructure and is not applicable to aspect ratio and fraction of elongated grains.

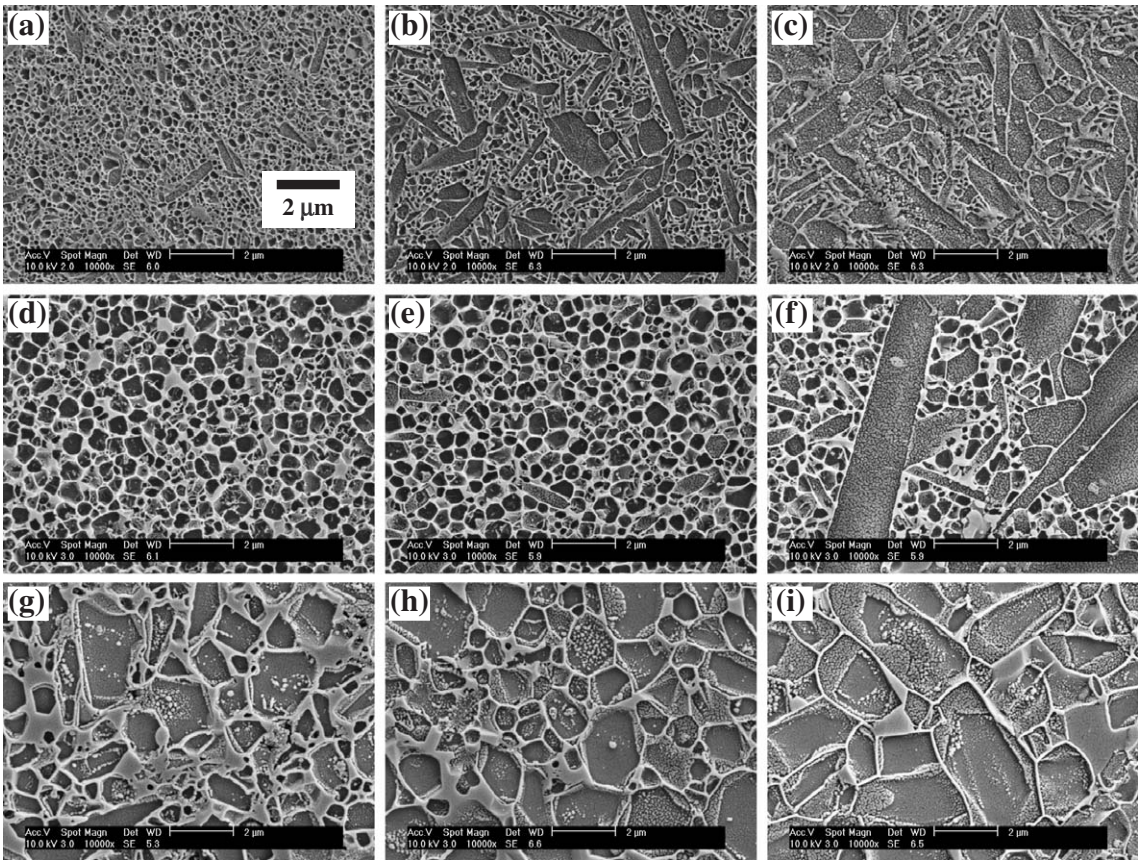

Fig. 3. The (a) F1, (b) F2, and (c) F3 belong to the Si_3N_4 sintered at 1600, 1700, and 1800 °C starting from a fine α phase powder, respectively. The (d) C1, (e) C2, and (f) C3 denote the Si_3N_4 sintered at 1600, 1700, 1800 °C starting from the coarse α phase, respectively. The (g) B1, (h) B2, and (i) B3 represent the Si_3N_4 sintered at 1600, 1700, and 1800 °C from the β phase, respectively.

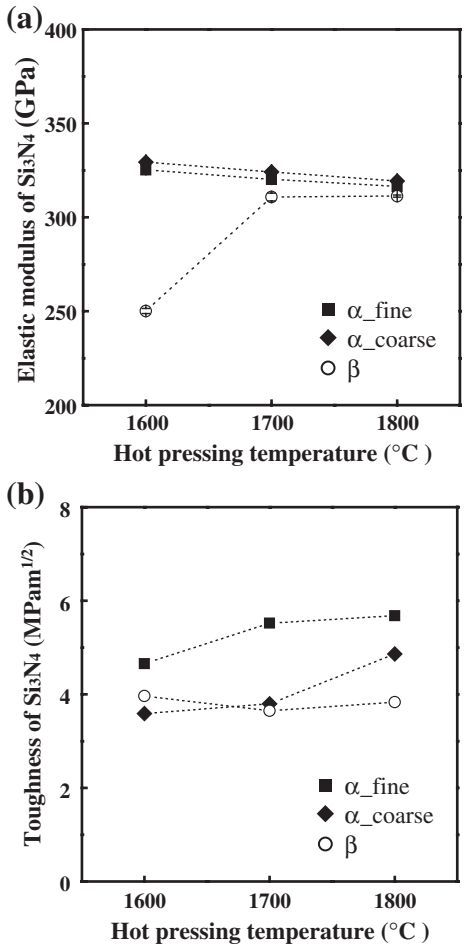

Fig. 4. Plot of (a) Young's modulus and (b) toughness of F, C and B Si_3N_4 substrate materials as function of hot-pressing temperature.

Characteristics of each Si_3N_4 were summarized in Table 2. The phase ratio of β-to-α increases as sintering temperature rises. The sintering process promotes the phase transformation of Si_3N_4 from the α to the stable β phase at high temperatures [19]. The silicon nitrides using coarse α phase powder show slower transformation from α to β than those using fine α powder. At 1800 °C, complete transformation to β was achieved in Si_3N_4 with fine α phase but only a 40% transformation occurred in Si_3N_4 with coarse α phase. Elongated grains increase fracture toughness through grain bridging and the crack deflection mechanism. Only grains which show an aspect ratio higher than 2 were chosen to measure aspect ratio. The aspect ratios of both Si_3N_4 substrates sintered with fine α and β phases show constant value through sintering temperature and the Si_3N_4 with a coarse α phase is linearly proportional to hot pressing temperature. At 1800 °C, Si_3N_4 having an aspect ratio higher than 5 was obtained for Si_3N_4 with α phase for both coarse and fine powder. On the contrary, almost all the equiaxed grains of Si_3N_4 were obtained from β powder. The volumetric ratio of elongated β increased with temperature. All Si_3N_4 except the specimen sintered at 1600 °C with β powder showed nearly full density of theoretical value.

The elastic modulus and toughness of Si_3N_4 were shown in Fig. 4. The elastic modulus of Si_3N_4 decreases slightly with sintering temperature, except for the Si_3N_4 sintered at 1600 °C with β powder. The elastic modulus of the three kinds of Si_3N_4 approaches that of Si_3N_4 with β at 1800 °C, and this saturation of elastic modulus value is consistent with higher content of β phase at higher temperature. The toughness of Si_3N_4 increases with temperature, and Si_3N_4 sintered with fine α phase showed the highest value over the temperature range. On the contrary, the toughness of Si_3N_4 started from the β phase was relatively low and constant with the changes in sintering temperature. The toughness enhancement of both Si_3N_4 substrates with fine and coarse α phase powder was mainly attributed to increase of elongated β grains with increases in temperature. No significant change in the toughness of the Si_3N_4 with β phase was due to the large and equiaxed grains with sintering temperature.

Hertzian indentation has been used as a powerful means to quantify damages in ceramics [28,29], including Si_3N_4 [17,30]. This method reveals, in a most compelling manner, the critical role of microstructure in the competition between classical cracking (ring, or cone fracture) and quasi-plastic damage (distributed shear-activated microfaulting). Distinctions between

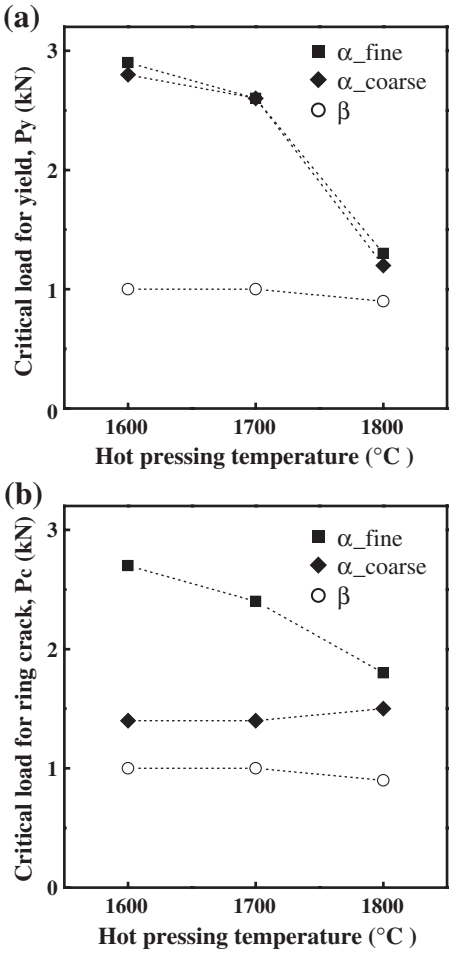

Fig. 5. The indentation damage response of Si_3N_4 in terms of P_y and P_c. (a) The critical load to initiate surface impression, P_y and (b) the critical load to make ring crack on Si_3N_4 surface, P_c.

these two damage modes are directly relevant to applications where highly concentrated loads occur. Indications occur when the damage mode in Si_3N_4 progresses from cracking to quasi-plasticity as the microstructure coarsens and elongates and as the β-to-α ratio increases [17,30]. In order to investigate the yield properties of Si_3N_4, Hertzian indentation was used. Indentation-induced damage as a function of hot pressing temperature was observed in the context of critical load for yield, P_y, and critical load for ring crack, P_c. P_y is defined as the initial load required to make an indentation impression on the surface and P_c as the load to make a ring crack on surface. P_y is a critical load for onset of surface impression in Hertzian contact, which represents the (quasi-plastic) yield characteristics of ceramics. The size of indentation impression depends on the test condition such as a radius of spherical indenter, load, and indenter/specimen materials. In this experiment, WC sphere with a radius of 1.98 mm was used and the size of impression was ranged from 50 to 200 μm in diameter. P_y was obtained from the initial load to induce first surface impression. The relationship between P_y and conventional hardness (H) have been suggested as $P_y \approx H(H/E')^2 r^2$, where E' and r' are the effective modulus and effective radius, respectively [31]. As the hot pressing temperature increased, P_y decreased for both Si_3N_4 substrates with fine and coarse α phase, as shown in Fig. 5(a). Such a decrease in P_y mainly results from the increase in grain size and ratio of elongated β phase; however, no significant change of P_y of the Si_3N_4 with β phase was observed. The critical load for yield, P_y, of Si_3N_4 with fine and coarse α phases, sintered at 1600 °C was very high (2.9 and 2.8 kN), respectively, and it decreased with temperature. The decrease of P_y was slow between 1600 and 1700 °C, but was more abrupt between 1700 and 1800 °C. This was due to the increase of the amount of the softer β phase with increase in temperature.

In case of the Si_3N_4 started from α phase powder, P_y showed very high value about 2.8 kN and decreased from 2.8 to 1.5 kN as grain size, β to α ratio increased. On the contrary, Si_3N_4 From β phase powder exhibited very low P_y about 1.0 kN and the value kept constant as grain size increased.

By controlling the starting powder and sintering temperature, Si_3N_4 substrates having microstructures with different ratios of β to α phase and different grain sizes, shapes, and volume fractions of each phase were fabricated. The adhesion strength of PVD TiN coating on the Si_3N_4 layered system related to TiN delamination and failure mode was investigated in the context of the microstructure of Si_3N_4 substrate.

3.2. The adhesion strength of TiN films coated on Si_3N_4

Characteristics of the deposited TiN film were evaluated in the point of phase, thickness, composition, elastic modulus, and hardness as shown in Fig. 6. In a preliminary study, deposition conditions such as the bias voltage, N_2 pressure, and substrate temperature were optimized from the standpoint

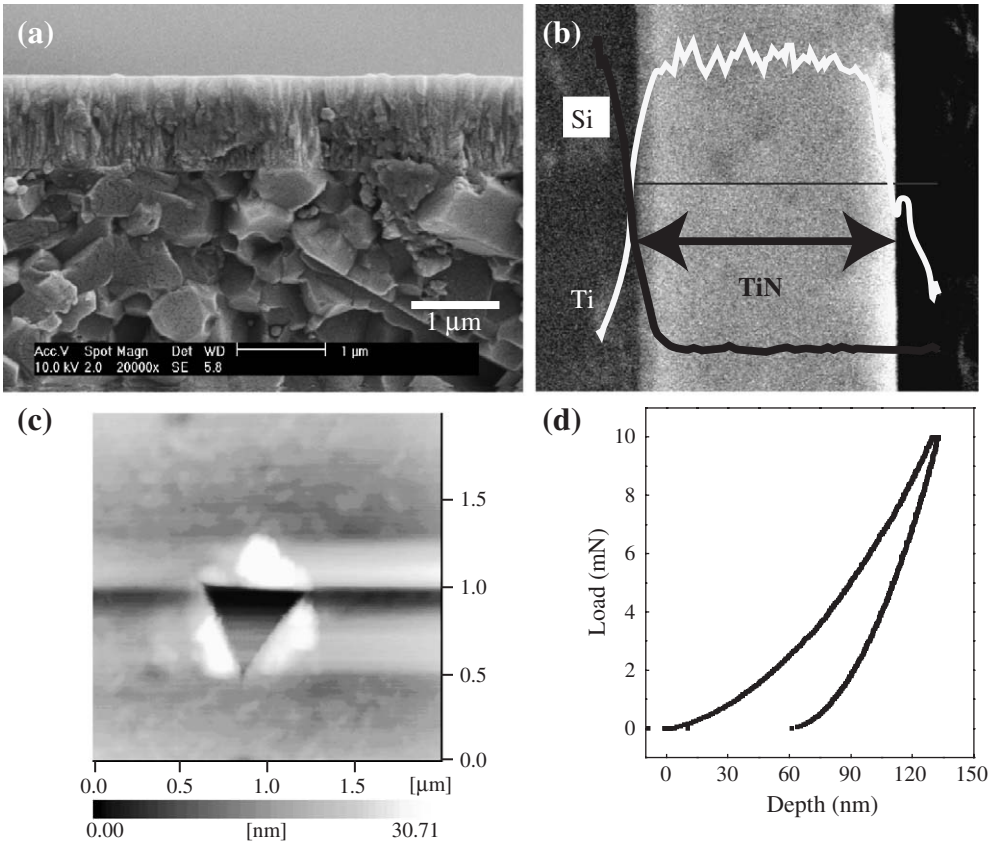

Fig. 6. (a) A SEM cross-sectional view of TiN film on C2-Si_3N_4, (b) the uniformity of TiN composition within the TiN thickness, (c) the surface impression after nano indentation at a maximum load of 10 mN using Berkovich tip of radius, r=100 nm, and (d) the load-displacement curve during nano indentation.

of the TiN phase which was analyzed by X-Ray Diffraction. The uniformity of TiN through whole thickness was confirmed by the distribution of Ti. Uniform level of Ti intensity indicates the uniform TiN distribution in the TiN coatings. TiN thickness was linearly proportional to deposition time. The deposition rate was slightly dependent on Si_3N_4 microstructure. Si_3N_4 with a higher fraction of α phase showed slightly more increased thickness 0.05 to 0.1 μm at the same deposition time than 1 μm thick TiN on Si_3N_4 with β phase. TiN on all the Si_3N_4 substrates was controlled to have 1 μm of thickness to exclude the effect of thickness on adhesion strength. Fig. 6(a) shows the SEM cross-sectional view, showing TiN coating on a Si_3N_4 substrate sintered at 1700 °C with coarse α powder. TiN film was clearly distinguished from the Si_3N_4 substrate. TiN thickness was determined as 1.08 μm. TiN composition was confirmed as shown in Fig. 6(b). The elemental distribution of Ti indicates a uniform TiN composition through the whole TiN coating. Fig. 6(c) shows a nano indentation-induced surface impression with a Berkovich tip at a maximum load of 10 mN, and the load-displacement curve during nano indentation was depicted in Fig. 6(d). A maximum penetration depth of less than 200 nm was maintained, one-fifth of the total TiN film thickness. There was no particular event, such as pop-in or pop-out during the loading or unloading procedure. The hardness and elastic modulus of TiN were evaluated according to the Oliver and Pharr procedure [32]. The hardness and elastic modulus of TiN film were 27.5±1.4 and 570±5.4 GPa, respectively. The TiN coating on different Si_3N_4 substrates was prepared for the evaluation of adhesion strength.

The adhesion strength of TiN film on Si_3N_4 was evaluated by a scratch test, which utilizes a spherical diamond indenter with a radius of 200 μm. As a reference, commercially available WC substrate was deposited by the same TiN film, and the adhesion strengths were compared. TiN/F1-Si_3N_4 showed the highest adhesion strength of 138±3.4 N among all TiN coatings on Si_3N_4. The adhesion strengths of TiN film on Si_3N_4 started from both of fine and coarse α powder were much higher than that of TiN on WC reference material (L_c=85 N). In TiN/α-Si_3N_4 specimens, adhesion strength decreased with the increasing sintering temperature of Si_3N_4 substrate. The decrease resulted from larger grain size and an increase of the amount of β phase as sintering temperature increased. On the contrary, in the case of TiN/β-Si_3N_4, relatively low adhesion strength was measured, and it was interpreted in the same context of full β content in Si_3N_4 substrate. However, the adhesion strength of TiN/β-Si_3N_4 was a comparable value with that of TiN/WC specimen.

Finally, adhesion strength was compared with substrate hardness in Fig. 7(b). The variation in the hardness of Si_3N_4 was very similar to that in the adhesion strength of TiN coating on Si_3N_4. Correlations between adhesion strength and substrate hardness have been reported in earlier studies for hard coatings on metallic substrate [4,14]. Interfacial delamination or TiN spallation can be induced by the deformation of a relatively soft substrate during a scratch, but it is interesting for a hard substrate, in this case Si_3N_4 ceramics, to show similar results

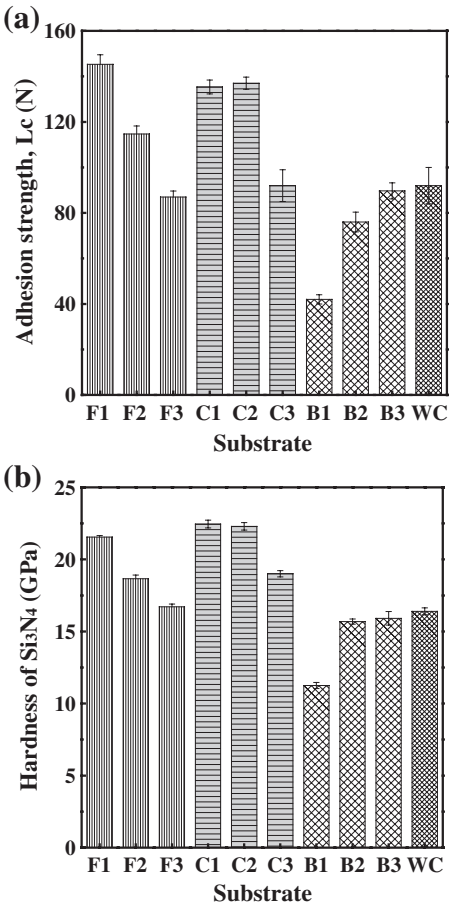

Fig. 7. (a) The adhesion strength of TiN film on Si_3N_4 and (b) the Vickers hardness of Si_3N_4 substrate. The TiN film on WC was chosen as a reference.

with a soft metallic substrate. Adhesion strength and substrate hardness showed a very close relationship in Fig. 7. This result implies substrate hardness strongly affects the adhesion strength, even in the case of hard ceramic substrate.

The adhesion strength of PVD TiN film on Si_3N_4 was affected by substrate properties, especially hardness and critical load for yield, P_y. Quasi-plasticity as well as hardness is probably related with damage response of ceramics considering that ceramics generally become deformed with the evolution of quasi-plasticity. The quasi-plastic damage of the Si_3N_4 substrate is evaluated by P_y in Hertzian indentation experiment. In this study, P_y and the hardness of the Si_3N_4 substrate were governed by Si_3N_4 microstructure. The grain size, β to α ratio, and aspect ratio of the Si_3N_4 substrate were controlled through sintering temperature and starting powder size and phase. Microstructures of Si_3N_4 showing higher adhesion strength have common features with the finer grain size and dominant α phase.

By controlling the microstructure of a substrate, quasi-plastic yield properties and hardness could be optimized to obtain higher adhesion strengths of TiN coating. In PVD TiN film on Si_3N_4 system, the Si_3N_4 substrate with a microstructure of finer grain size and higher α phase is desirable for maximizing adhesion strength. The PVD TiN coating on Si_3N_4 is highly expected to show great performance in the application fields of

cutting tools and bearings considering the high adhesion strength.

4. Conclusion

The effect of Si_3N_4 microstructure on the adhesion strength of PVD TiN film to the Si_3N_4 substrate was investigated. The adhesion strength of TiN coating was strongly influenced by microstructure-controlled Si_3N_4 substrate properties. A strong correlation between the adhesion strength and the hardness of the ceramic substrate was observed. The quasi-plastic yield properties of the Si_3N_4 substrate were interpreted as a failure or delamination source of TiN films. By controlling the microstructure of a substrate, quasi-plastic yield properties and hardness of Si_3N_4 could be optimized to maximize the adhesion strength of TiN coating. Si_3N_4, substrates with finer grain sizes and higher α phase ratios, which show high hardness and high P_y, were suitable for higher adhesion strength of TiN film.

Acknowledgements

This work was supported by a grant for International Collaboration Research Program from Korea Ministry of Science and Technology (M6-0105-00-0012).

References

[1] M. Stoiber, E. Badisch, C. Lugmair, C. Mitterer, Surf. Coat. Technol. 163–164 (2003) 451.
[2] Y.M. Chen, G.P. Yu, J.H. Huang, Surf. Coat. Technol. 155 (2002) 239.
[3] A. Kuper, R. Clissold, P.J. Martin, M.V. Swain, Thin Solid Films 308–309 (1997) 329.
[4] M. Larsson, M. Bromark, P. Hedenqvist, S. Hogmark, Surf. Coat. Technol. 76–77 (1996) 202.
[5] F.S. Shieu, L.H. Cheng, Y.C. Sung, J.H. Huang, G.P. Yu, This Solid Films 334 (1998) 125.
[6] H.C. Chen, B.H. Tseng, M.P. Houng, Y.H. Wang, Thin Solid Films 445 (2003) 112.
[7] K. Chen, Y. Yu, H. Mu, Surf. Coat. Technol. 151–152 (2002) 434.
[8] M. Moriyama, T. Kawazoe, M. Tanaka, M. Murakami, Thin Solid Films 416 (2002) 136.
[9] H.E. Cheng, M.H. Hon, Surf. Coat. Technol. 81 (1996) 256.
[10] L. Karlsson, L. Hultman, J.E. Sundgren, Thin Solid Films 371 (2000) 167.
[11] F.S. Shieu, L.H. Cheng, M.H. Shiao, S.H. Lin, Thin Solid Films 311 (1997) 138.
[12] A. Alsaran, Mater. Sci. Eng., A Struct. Mater.: Prop. Microstruct. Process. 371 (2004) 141.
[13] M.H. Shiao, S.A. Kao, F.S. Shieu, Thin Solid Films 375 (2000) 163.
[14] A. Rodrigo, P. Perillo, H. Ichimura, Surf. Coat. Technol. 124 (2000) 87.
[15] Y.-G. Kim, D.K. Kim, J. Mater. Res. 20 (2005) 1389.
[16] S.K. Lee, K.S. Lee, B.R. Lawn, D.K. Kim, J. Am. Ceram. Soc. 81 (1998) 2061.
[17] S.K. Lee, S. Wuttiphan, B.R. Lawn, J. Am. Ceram. Soc. 80 (1997) 2367.
[18] M. Mitomo, S. Uenosono, J. Am. Ceram. Soc. 75 (1992) 103.
[19] F.F. Lange, J. Am. Ceram. Soc. 62 (1979) 428.
[20] R.N. Katz, Mater. Res. Soc. Symp. Proc. 287 (1992).
[21] C. Liu, Mater. Sci. Eng., A Struct. Mater.: Prop. Microstruct. Process. 363 (2003) 221.
[22] M. Bracisiewicz, V. Medri, A. Bellosi, Appl. Surf. Sci. 202 (2002) 139.
[23] S. Guicciardi, C. Melandri, V. Medri, A. Bellosi, Mater. Sci. Eng., A Struct. Mater.: Prop. Microstruct. Process. 360 (2003) 35.
[24] P. Sajgalik, J. Dusza, M.J. Hoffmann, J. Am. Ceram. Soc. 78 (1995) 2619.
[25] Standard Test Method for Dynamic Young's Modulus, Shear Modulus, and Poisson's Ratio for Advanced Ceramics by Impulse Excitation of Vibration, American Society for Testing and Materials, Standard C 1259-01, 2001.
[26] G.R. Chantikul, B.R. Lawn, J. Am. Ceram. Soc. 64 (1981) 533.
[27] B.R. Lawn, J. Am. Ceram. Soc. 81 (1998) 1977.
[28] H. Cai, M.A.S. Kalceff, B.R. Lawn, J. Mater. Res. 9 (1994) 762.
[29] F. Guiberteau, N.P. Padture, H. Cai, B.R. Lawn, Philos. Mag., A 68 (1993) 1003.
[30] H.H.K. Xu, S. Jahanmir, L.K. Ives, J. Mater. Sci. 30 (1995) 869.
[31] Y.-W. Rhee, H.-W. Kim, Y. Deng, B.R. Lawn, J. Am. Ceram. Soc. 84 (2001) 561.
[32] W.C. Oliver, G.M. Pharr, J. Mater. Res. 7 (1992) 1564.